arXiv:cond-mat/0206072v1 [cond-mat.mtrl-sci] 6 Jun 2002

High magnetic field transport measurement of charge-ordered $Pr_{0.5}Ca_{0.5}MnO_3$ strained thin films.

W. Prellier*,[1], E. Rauwel Buzin[1], S. de Brion[2], G. Chouteau[2], Ch. Simon[1], B. Mercey[1] and M. Hervieu[1]

[1] *Laboratoire CRISMAT, CNRS UMR 6508, Bd du Maréchal Juin, F-14050 Caen Cedex, France*

[2] *Grenoble High Magnetic Field Laboratory, CNRS and MPI-FKF, BP 166, 38042 Grenoble Cedex 9, France.*

(March 22, 2022)

Abstract

We have investigated the magnetic-field-induced phase transition of charge-ordered (CO) $Pr_{0.5}Ca_{0.5}MnO_3$ thin films, deposited onto (100)-oriented $LaAlO_3$ and (100)-oriented $SrTiO_3$ substrates using the pulsed laser deposition technique, by measuring the transport properties with magnetic fields up to 22T. The transition to a metallic state is observed on both substrates by application of a critical magnetic field ($H_C > 10T$ at $60K$). The value of the field required to destroy the charge-ordered insulating state, lower than the bulk compound, depends on both the substrate and the thickness of the film. The difference of the critical magnetic field between the films and the bulk material is explained by the difference of in-plane parameters at low temperature (below the CO transition). Finally, these results confirm that the robustness of the CO state, depends mainly on the stress induced by the difference in the thermal dilatations between the film and the substrate.

*prellier@ismra.fr

For the past years, there has been a large focus on the charge ordering (CO) and orbital ordering (OO) phenomena[1] in transition metal oxides. Interesting compounds showing this behavior include manganite oxides, such as $Nd_{0.5}Sr_{0.5}MnO_3$[2], $Pr_{1-x}Ca_xMnO_3$[3], or nickelates like $La_{2-x}Sr_xNiO_4$[4]. In colossal magnetoresistive (CMR) manganites[5], charge/orbital ordering corresponds to an ordering of the charges/orbitals in two different Mn sublattices (i.e. a long-range ordering of Mn^{3+} and Mn^{4+} ions). It appears for certain value of x and particular average cation radius. Under cooling, the polaronic transport in the paramagnetic state becomes unstable, below a certain temperature (T_{CO}) and the material goes to an insulating, charge-ordered (CO) state. T_{CO} decreases with increasing field[6]. The feature that the charge-ordering can be destroy leading to metallic-like state, under the application of an external perturbation like magnetic field[2,3], electric field[7], visible-infrared light[8], electron irradiation[9] or X-rays[10] has stimulated extensive work with the aim of examining complex structural and magnetotransport transitions. Interestingly, this fall of resistivity much larger than the conventional CMR materials[11], has increased their potential use for technologic applications. However, prior to a routine utilization, we need to correctly control the thin films growth[12] and their characterizations.

For these reasons, we have first undertaken studies on $Pr_{0.5}Ca_{0.5}MnO_3$ (PCMO) films deposited on $LaAlO_3$[13] and $SrTiO_3$[14,15] substrates in order to understand the effect of substrate-induced strains. While the thinner films do not exhibit any temperature induced insulator-metal transition under an applied magnetic field up to $9T$, for thickness larger than $110nm$ a $5T$ magnetic field is sufficient to destroy the CO/OO state[15]. This indicates that strains play a crucial role in the stability of the CO/OO state. These previous studies, limited to $9T$, were not very conclusive on the origin of this effect since the CO/OO state of the thinner films and of the bulk material do not collapse under a $9T$ magnetic field. Note that a magnetic field of $25T$ (at $4K$) is required to destroy this insulating state in bulk $Pr_{0.5}Ca_{0.5}MnO_3$[16].

In the present work, we have studied the magnetic-field-induced phase transition of CO/OO $Pr_{0.5}Ca_{0.5}MnO_3$ films in high magnetic fields up to $22T$. We have carried out

transport measurements over a wide temperature range for two types of samples where any effect was seen up to $9T$: a $25nm$ film grown on $SrTiO_3$ (STO) and a $250nm$ film deposited on $LaAlO_3$ (LAO)[13,14]. Based on these results, we have determined the dependence of the critical magnetic field as a function of temperature and as a function of the film thickness and compared it to what is observed in the bulk compound. Finally, we have correlated this mechanism with the structural properties of the thin films.

Thin films of PCMO were grown in-situ using the pulsed laser deposition technique on (100)-$LaAlO_3$ (pseudocubic with $a = 0.3788nm$) and (100)-$SrTiO_3$ (cubic with $a = 0.3905nm$) substrates. Detailed optimization of the growth procedure was completed and described previously[13,14]. The structural study was carried out by X-Ray diffraction (XRD) using a Seifert XRD 3000P at room temperature (Cu Kα, $\lambda = 0.15406nm$). Resistivity (ρ) was measured by a four-probe method as a function of the magnetic field (H) up to $22T$, for various temperature (T) in the range $4 - 300K$. The speed of the field used, in ramping up and down, was $25mT/sec$ (we also measured the PCMO film on STO with a speed of $55mT/s$ and $85mT/s$ but no changes were observed). The composition of the films was checked by energy-dispersive spectroscopy analyses. It is homogenous and corresponds exactly to the composition of the target (i.e.$Pr_{0.5\pm0.02}Ca_{0.5\pm0.02}Mn$) in the limit of the accuracy.

Fig.1 shows a typical $\theta - 2\theta$ scan recorded for a film of $25nm$ film on STO (Fig.1a) and $250nm$ film on LAO (Fig.1b). As already reported, the film is a single phase, [010]-oriented (i.e. with the [010] axis perpendicular to the substrate plane) on STO and [101]-oriented on LAO (i.e. with the [101] axis perpendicular to the substrate plane in the space group $Pnma$[18] and we have attributed this surprising orientation as a result of the lattice mismatch between the film and the substrate[15]. The out-of-plane parameter, at room temperature, is $0.376nm$ for the $25nm$ film grown on STO substrate and $0.384nm$ for the $250nm$ film deposited on LAO substrate confirming that the PCMO film is under expansion in the plane of STO and under compression in-the-plane of LAO, respectively.

The magnetic-field dependence of the resistivity at various temperatures for $Pr_{0.5}Ca_{0.5}MnO_3$ film on STO substrate is shown on Fig.2. The resistivity shows a huge

decrease on a logarithmic scale, showing the transition toward the charge disordered, metallic phase. We define the critical field H_C for this phase transition at the inflection point. There is a strong hysteresis between the field-increasing (H_C^+) and field-decreasing (H_C^-) behavior as observed in the bulk material but the values are very different. For instance, the critical field at 120K is close to $15T$ for the $25nm$ film on STO, whereas in the bulk compound, H_C is around $22T$[16].

The in-plane misfit $\sigma = 100 * (a_F - a_B)/a_B$ (where a_F is the in-plane parameter of the film and a_B is the lattice parameter of bulk PCMO) is calculated at room temperature. a_B corresponds to the d_{101} in the case of STO and to the d_{010} in the case of LAO respectively, due to the different orientation of the film with respect to the substrate. The evolution of the critical magnetic field as a function of this misfit, at room temperature, is presented Fig.3a. At $T = 300K$, there is no clear correlation between these two parameters. In particular, the value of H_C tends, for the highest thicknesses of the films on STO substrates, to a value which is completely different from that of the bulk material. We have already discussed in previous papers the possible explanation in terms of changes of the composition or in the oxygen content: this explanation was ruled out completely by the fact that the structural parameters relaxes to the bulk value when the film is removed from the substrate by scratching[13]. In particular the modulation vector[19], q, of the CO/OO state which is 0.48 in the bulk stoichiometric sample is only 0.38 in one of the film on LAO substrates. After scratching (i.e. when the film is substrate-free), it comes back to the bulk value of 0.48[13] indicating that the value of 0.38 is only a result of the substrate-induced strains.

The interpretation that we propose is that, when the film remains epitaxial on the substrate, the CO state cannot fully develop because it is impossible to accommodate the quite large change in the structural parameters occurring below T_{CO} in the bulk[20]. For example, in the bulk PCMO, the [101] lattice parameter (which should be compared to the in-plane parameter on STO) is going from $0.382nm$ to $0.386nm$ in the CO state. Since the low temperature ED study has shown that the film remains epitaxial below the CO transition, the in-plane lattice parameter of the film cannot reach $0.386nm$ and remains

close to the substrate value ($0.390nm$) for the thinner film.

For the thicker films, at the synthesis temperature, the in-plane lattice parameters relax smoothly across its thickness (t) from the STO value to a value $0.381nm$ close to the bulk one. At room temperature, the values are slightly smaller but remains almost unchanged ($0.390nm$ and $0.381nm$ for the substrate and the film respectively). For characterizing the nanostructural state of the films and, more especially, understanding the way the relaxation is ensured as the thickness increases, an electron diffraction (ED) and high resolution electron microscopy (HREM) study was carried out on the thicker film ($t > 200nm$). The study was performed with a TOPCON 002B electron microscope having a $0.18nm$ point to point resolution ($Voltage = 200kV$ and spherical aberration coefficient $C_S = 0.4mm$). The ED patterns confirm that the whole film is [010]-oriented and evidence also the existence of twinning domains. Such domains, resulting from the orthorhombic distortion of the perovskite subcell, have been extensively described[21]. The original character of the present film, by opposition to the bulk and certain films[22]) is that only two variants out of six are observed, namely those with the [100] and [001] directions parallel the $\{110\}_{STO}$ equivalent directions. These points are illustrated in Fig.4a (only one quadrant of the ED pattern is given for allowing a sufficient enlargement) and in the HREM image in Fig.4c. These ED patterns provide two other important informations. First, the 600 and 006 reflections of the film are perfectly superimposed showing that the a and c parameters are equal. The through focus HREM series confirmed the homogeneity of the film structure (in agreement with the simulated images, calculated with a Mc TEMPAS software). Second, the conditions of reflection ($Pnma$ space group) show that the symmetry of the cell remains orthorhombic despite this particular geometrical relationship imposed by the substrate, i.e. the tilting mode of the octahedra is similar to that of the bulk material.

The overall images of the film (Fig.4b) show alternating broad dark and bright bands perpendicular to the substrate plane, which are characteristic of strain effects (and associated to the relaxation mode). The evolution of the a, b and c parameters throughout the films,

was determined by measuring directly on the HREM images, taking those of the substrate as references[23]. It shows that, concomitantly and continuously, a (and c, since $a = c$) increases whereas b decreases when going away from the interface. This evolution is made at roughly constant cell volume (in the limit of accuracy of the measurements). Large areas of the film were carefully investigated. No dislocation has been detected, whatever the film zone, ruling out definitely such a structural mechanism for explaining the relaxation. The detailed examination (reported elsewhere) allows a mechanism of smooth variation to be proposed. The images indeed show very local variations of the contrast. They appear as point like defects and waving atomic rows, associated to ion displacements and local distortions of the octahedra. This is exemplified in film areas very close to the interface (circled in Fig. 4c); the effect is clearly visible by viewing at grazing incidence. These phenomena are observed in the whole film and generate a tiny mosaicity of the film, responsible of the stripe-like contrast in the images (Fig.4b).

In conclusion, the electron microscopy study showed that the film exhibits the same $GdFeO_3$-type structure (orthorhombic-$Pnma$ space group) as the corresponding bulk material but with different lattice parameters and, consequently, different inter-atomic distances and inter-bond angles (in particular Mn-O distances and Mn-O-Mn angles). This effect is moreover accentuated by the strain effects, which are directly correlated to the in-plane misfit.

One would thus expect that the effect of the in-plane mismatch is more crucial below the CO temperature than at room temperature. Thus, we did the calculations of the mismatch at $120K$, a temperature below T_{CO}. For this, we consider that the in-plane parameters of the films have a tiny variation under cooling when going from $300K$ to $120K$ since the lattice parameters of the substrate is almost constant[24]. The resulting graph, calculated for STO substrates, is presented in Fig.3b. When the misfit is equal to zero (corresponding to the bulk value), the critical field is around $20T$[16]. It appears to be a maximum since a value of -0.5 (corresponding to a $110nm$ film) leads to a H_C of $5T$ whereas a value of $+0.5$ (corresponding to a $25nm$ film) gives a H_C of $17T$. We also add in this graph the datas of

LAO substrate calculated in the same way. However, it seems difficult to compare the results on LAO with STO since the films behave differently (nature of the strains, orientation of the film with respect to the substrate).

A $250nm$ thick film of PCMO grown on LAO was also investigated. Fig.5 shows the magnetic-field dependence of the resistivity at various temperatures. At $120K$, H_C is close to $10T$ which is also much lower than the bulk value. In order to compare these datas with films grown on STO, we are currently undertaken studies of films on LAO with various thickness.

One remark should also be made. H_C is always smaller in the case of the thin film. This means that the nature of the strains (i.e. compression or expansion) always drives H_C in the same direction due to the fact that the CO/OO state is less stable in a thin film. In others words, the CO/OO state is less established and it is easier to collapse it. This can be explained regarding the orientation of the film. On STO, the [010]-axis (corresponding to the out-of-plane direction) is compressed whereas the [101]-axis (corresponding to the in-plane direction) is expanded. On LAO, the [101]-axis is also compressed but this effect occurs in-the-plane of the substrate. Thus, the expansion of the [010]-axis destabilizes the orbital-ordering phase as seen in bulk $Nd_{1-x}Sr_xMnO_3$ where a compression of the [010]-axis assists the cooperative Jahn-Teller distortion and stabilizes the orbital-ordering state[25]. The difference of the H_C values between LAO and STO is due to the different mismatches between both substrates but the effect is similar.

In conclusion, the main parameter to control the CO/OO state is the low temperature in-plane parameter. When it reaches a value far from the bulk value, the CO/OO state cannot fully develop. This can be seen on the modulation vector parameter as it was previously published, but also, as it is found here, on the stability energy of the phase which can be directly calculated from the critical field (by multiplication by the moment of the ions). On STO substrate, the compression of the [010]-axis is measured. On LAO substrate, the same effect is observed along the [101]-axis.

We acknowledge Prof. B. Raveau, Dr. A. Maignan and Dr. A. Ambrosini for fruitful

discussions and carefull reading of the article.

REFERENCES

[1] Y. Tokura and N. Nagaosa, Science 288, 462 (2000).

[2] H. Kuwahara, Y. Tomioka, A. Asamitsu, Y. Moritomo and Y. Tokura, Science 270, 961 (1995).

[3] Y. Tomioka, A. Asamitsu, H. Kuwahara, Y. Moritomo, Y. Tokura, Phys. Rev. B 53, R1689 (1996).

[4] S.W. Cheong, H.Y. Hwang, C.H. Chen, B. Batlog, L.W. Rupp and S.A. Carter, Phys. Rev. B 49, 7088 (1994).

[5] For a reiview see: Colossal Magnetoresistance, Charge ordering and Related Properties of Manganese oxides, Edit. C.N.R. Rao and B. Raveau, World Scientific, Singapore, 1998.

[6] C.N.R. Rao, A. Arulraj, A.K. Cheetham and B. Raveau, J. Phys.: Condens. Matter. 12, R83 (2000).

[7] C.N.R. Rao, A.R. Raju, V. Ponambalam, S. Parashar and N. Kumar, Phys. Rev. B 61, 594 (2000), J. Stankiewicz, J. Sevé, J. Garcia, J. Blasco and C. Rillo, *idib.* 61, 11236 (2000), S. Srivastava, N.K. Pandey, P. Padhan and R.C. Budhani, *idib.* 62, 13868 (2000)

[8] K. Miyano, T. Tanaka, Y. Tomioka and Y. Tokura, Phys. Rev. Lett. 78, 4257 (1997), M. Baran, S.L. Gnatchenko, O. Gorbenko, A.R. Kaul, R. Szymczak and H. Szymczak, Phys. Rev. B 60, 9244 (1999).

[9] M. Hervieu, A. Barnabé, C. Martin, A. Maignan and B. Raveau, Phys. Rev. B 60, R726 (1999).

[10] V. Kiryukhin, D. Cas, J.P. Hill, B. Keimer, A. Vigliante, Y. Tomioka and Y. Tokura, Nature 386, 813 (1997), D.E. Cox, P.G. Radaelli, M. Marezio and S.W. Cheong, Phys. Rev. B 57, 3305 (1998).

[11] Doped manganites in this case refer to $La_{1-x}(Ca, Sr)_xMnO_3$, the so-called CMR materials

described by S. Jin, T.H. Tiefel, M. McCormack, R.A. Fastnacht, R. Ramesh and L.H. Chen, Science 264, 413 (1994).

[12] For a review see: W. Prellier, Ph. Lecoeur and B. Mercey, J. Phys.: Condens. Matter. 13, R915 (2001).

[13] A.M. Haghiri-Gosnet, M. Hervieu, Ch. Simon, B. Mercey and B. Raveau, J. Appl. Phys. 88, 3545 (2000).

[14] W. Prellier, A.M. Haghiri-Gosnet, B. Mercey, Ph. Lecoeur, M. Hervieu, Ch. Simon, and B. Raveau, Appl. Phys. Lett. 77, 1023 (2000).

[15] W. Prellier, Ch. Simon, A.M. Haghiri-Gosnet, B. Mercey and B. Raveau, Phys. Rev. B 62, R16337 (2000).

[16] M. Tokunaga, M. Miura, Y. Tomioka and Y. Tokura, Phys. Rev. B 57, 5259 (1998).

[17] Y. Ogimoto, M. Izumi, T. Manako, T. Kimura, Y. Tomioka, M. Kawasaki and Y. Tokura, Appl. Phys. Lett. 78, 3505 (2001).

[18] The structure of bulk PCMO is orthorhombic ($Pnma$) with $a = 0.5395nm$, $b = 0.7612nm$ and $c = 0.5403nm$ according to Z. Jirak, S. Krupicka, Z. Simsa, M. Doulka and S. Vratislma, J. Magn. Magn. Mat. 53, 153 (1985).

[19] The charge-orbital modulation vector q exhibits a value of $q = 1/2 - \epsilon$ where the incommensurability (ϵ) is zero for a perfect 1:1 charge-ordering.

[20] C. Martin, A. Maignan, F. Damay, M. Hervieu, B. Raveau, Z. Jirak, G. André, F. Bourée, J. Magn. Magn. Mat. 202, 11 (1999).

[21] M. Hervieu, G. Van Tendeloo, V. Caignert, A. Maignan and B. Raveau, Phys. Rev. B 53, 14274 (1996), B. Mercey, J. Wolfman, W. Prellier, M. Hervieu, Ch. Simon and B. Raveau, Chem. Mater. 12, 2858 (2000).

[22] O. I. Lebedev, G. Van Tendeloo, S. Amelinckx, B. Leibold and H.-U. Habermeier, Phys.

Rev. 58, 8065 (1998), F. S. Razavi, G. Gross, H.U. Habermeier, O. Lebedev, S. Amelinckx, G. Van Tendeloo, A. Vigliante, Appl. Phys. Lett. 76, 155 (2000).

[23] The STO substrate was used as a reference by measuring the distance between two dots, which corresponds a known unit cell ($0.3905nm$), away from the interface to avoid any local distortion . The lattice parameters of the film were measured in the same way, taking the distance between two dots which corresponding to a known integral number of unit cells.

[24] K.A. Muller, W. Berlinger and F. Waldner, Phys. Rev. Lett. 21, 814 (1968).

[25] T. Arima and K. Nakamura, Phys. Rev. B 60, R15013 (1999).

Figure Captions

Fig.1 : Room temperature $\theta - 2\theta$ XRD pattern of a PCMO thin film (a): $25nm$ on $SrTiO_3$, (b): $250nm$ on $LaAlO_3$.

Fig.2: $\rho(H)$ at different temperatures for a $25nm$ PCMO thin films grown on $SrTiO_3$. Runs in field increasing and decreasing are indicated by arrows.

Fig.3: Evolution of the critical magnetic field taken at $120K$, as a function of the in-plane misfit for different films (squares: STO, triangles: LAO) calculated (a): at room temperature (full symbols) and (b): below T_{CO} (empty symbols). Note the shift of the line at zero (corresponding to the bulk material) between $T = 300K$ and $T < T_{CO}$. The dashed and dots lines are only a guide for the eyes (see text for details).

Fig. 4a: ED of a cross-section for a PCMO/STO showing the [010]-axis perpendicular to the substrate plane. The spots allow an orthorhombic symmetry of the film, as seen in the bulk, but since the 600 and 006 reflections of the film are perfectly superimposed; this results in $a = c$. Subscripts F and S correspond to the substrate and the film respectively.

Fig. 4b: Overall cross-section image (bright field) of a PCMO film on STO showing the contrast typical of strain effects.

Fig. 4c: Cross-section (bright field) HREM image taken close to the interface film/substrate. No change of the lattice parameters are visible at the interface (marked by white arrows). The white circles (one is exemplified on the top of the image) show a local variation of the contrast. This variations indicate local distortions of the cell and waving atomic rows resulting of the smooth relaxation of the films due to the strains. Subscripts F and S correspond to the substrate and the film respectively.

Fig.5: $\rho(H)$ at different temperatures for $250nm$ PCMO thin films grown on $LaAlO_3$. Runs in field increasing and decreasing are indicated by arrows.

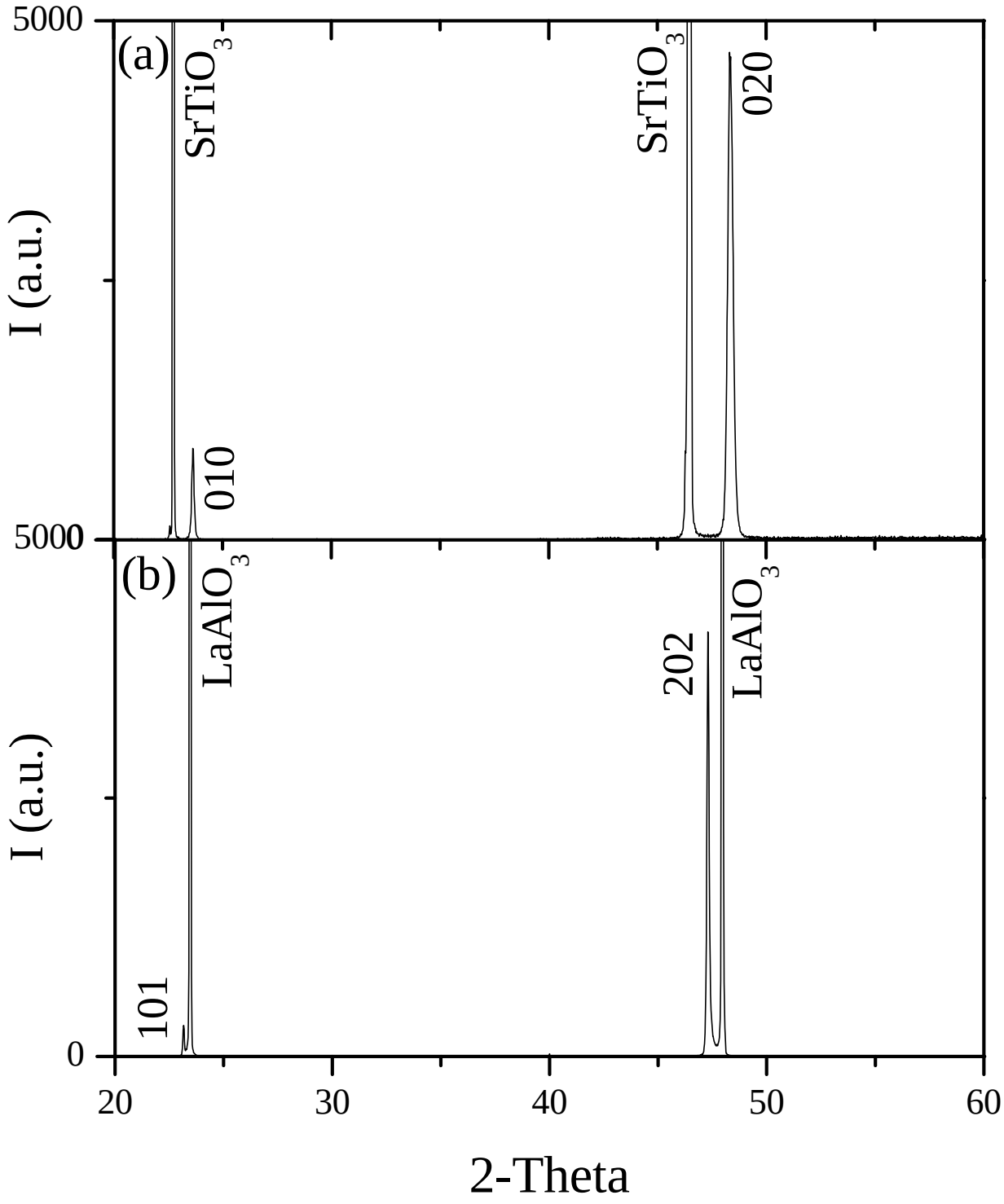


Figure 1

W. Prellier et al.

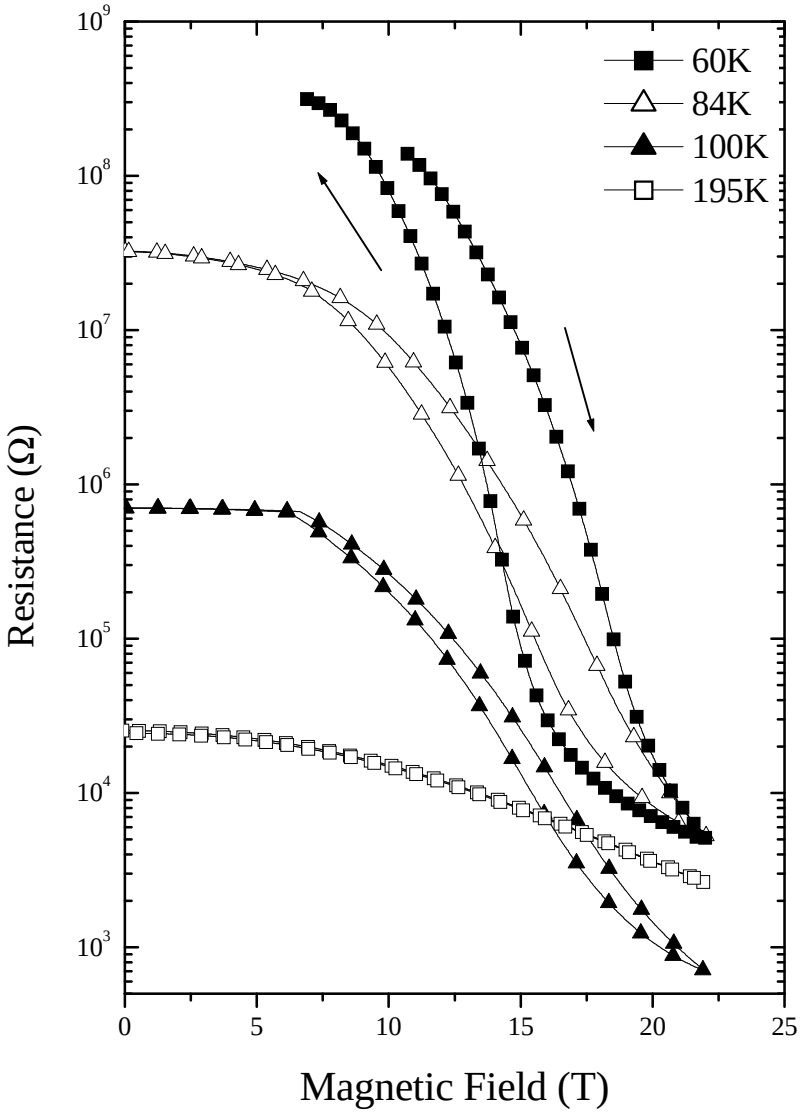


Figure 2

W. Prellier et al.

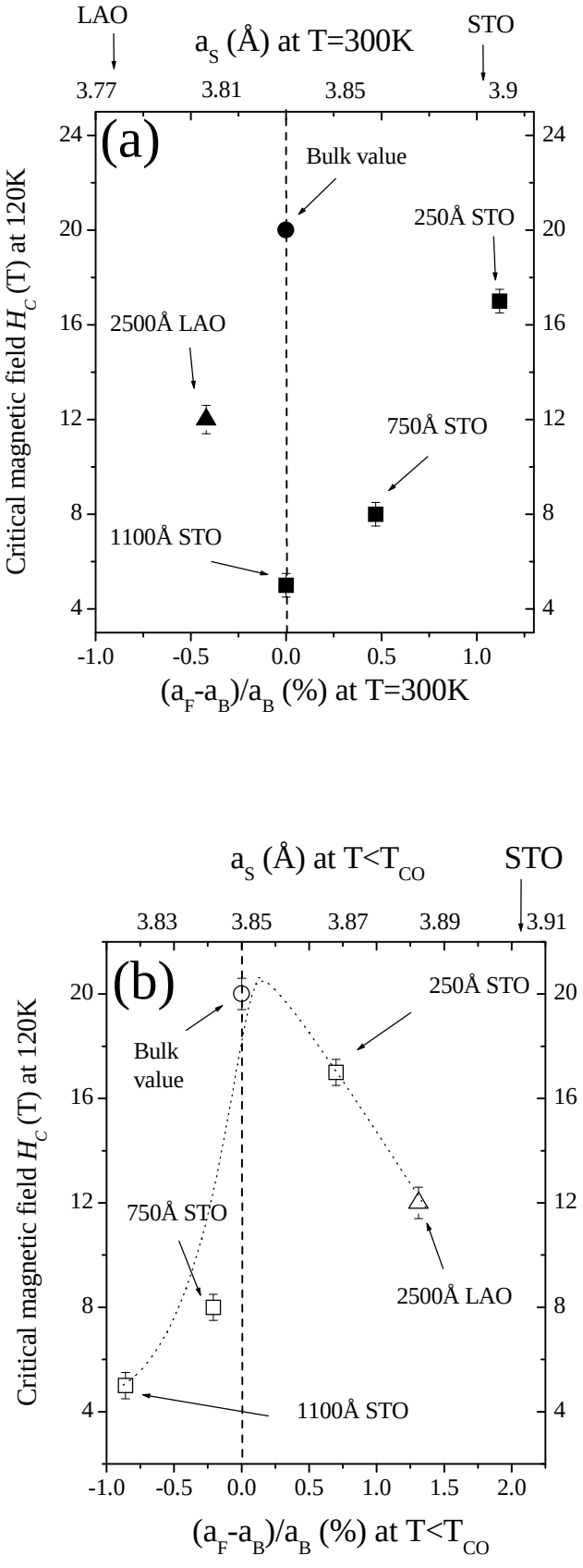


Figure 3 *W. Prellier et al.*

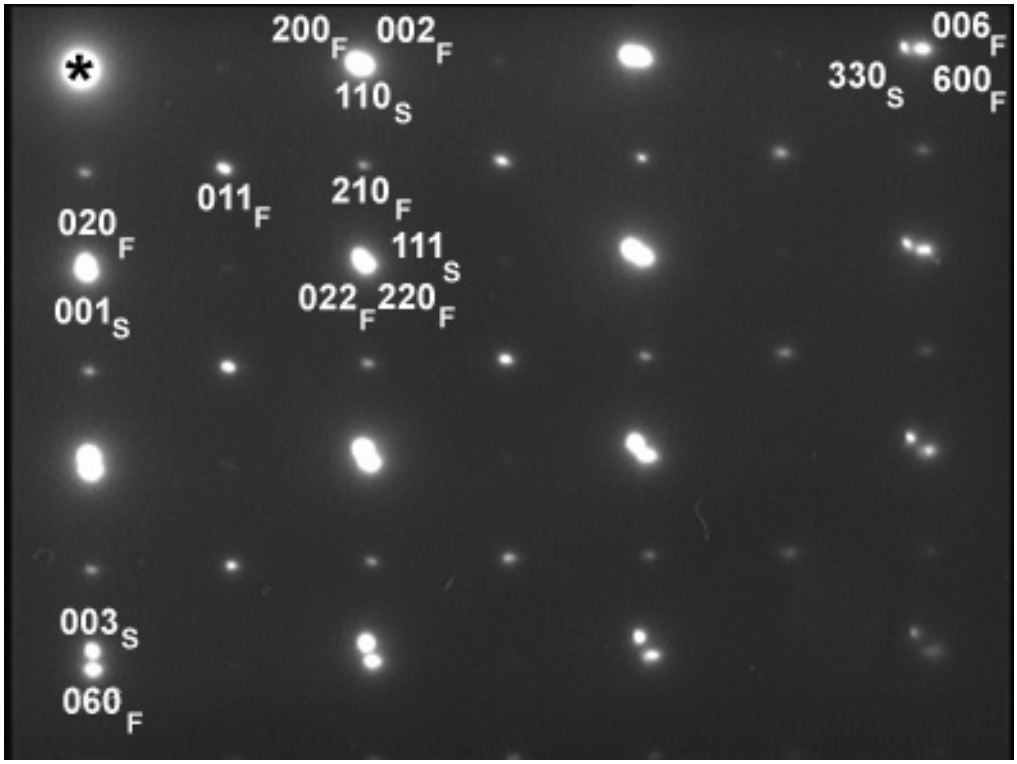


Figure 4a

W. Prellier et al.

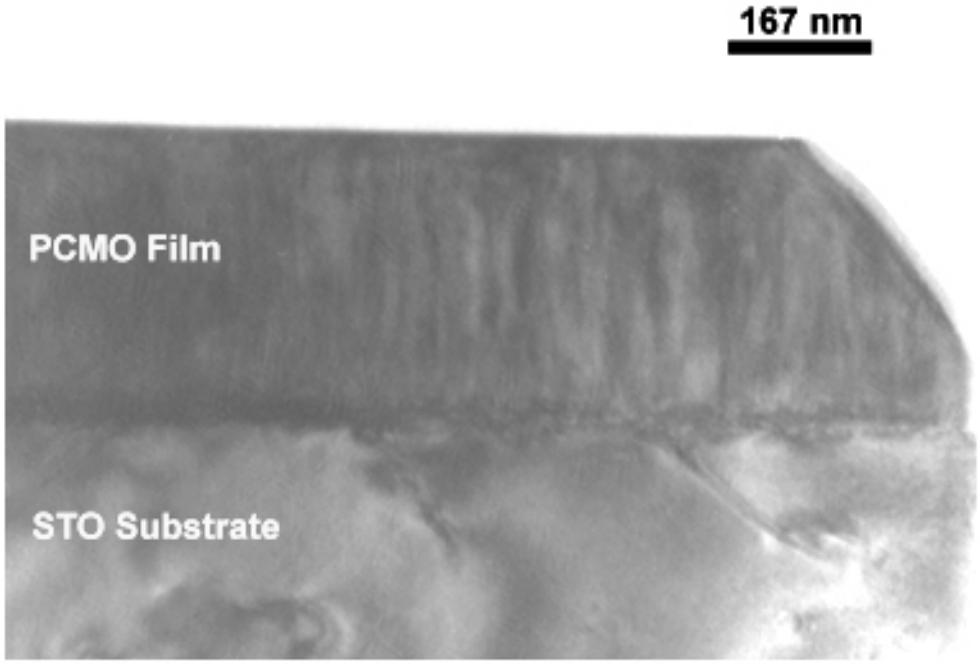


Figure 4b

W. Prellier et al.

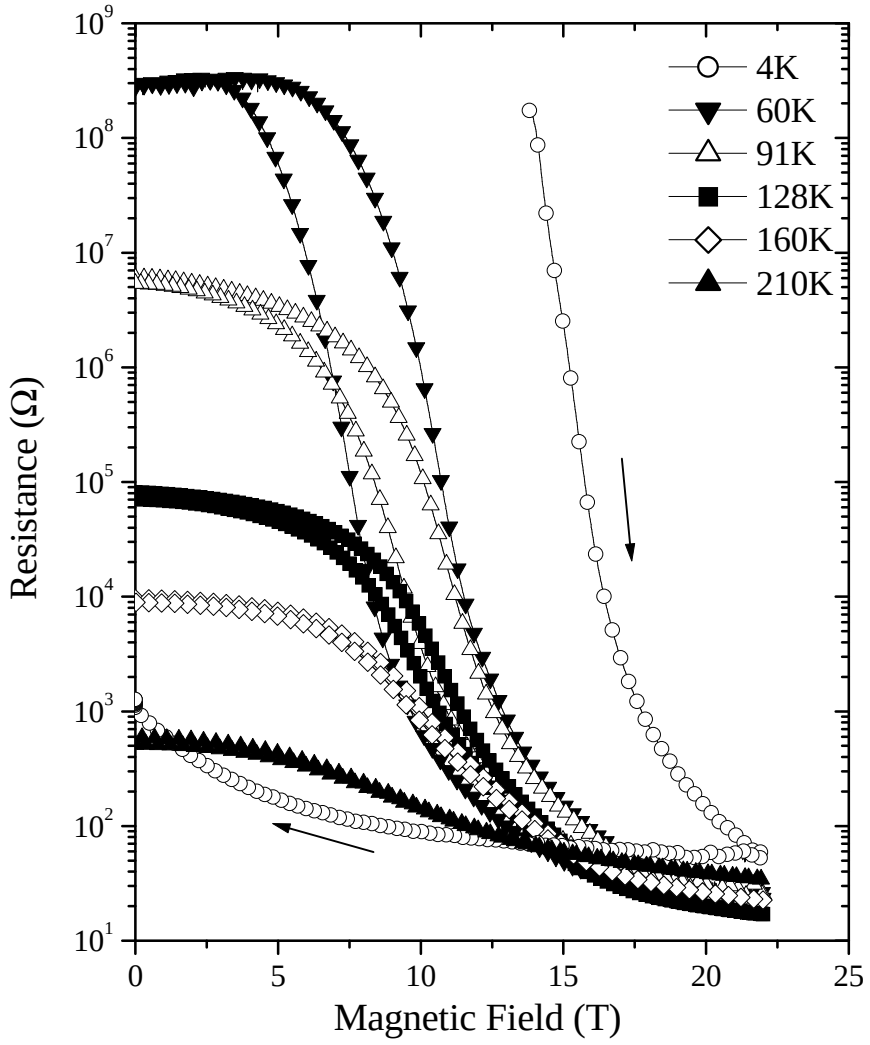


Figure 5

W. Prellier et al.